

Spaceborne evidence that ice-nucleating particles influence cloud phase

Tim Carlsen¹, Robert O. David^{1*}

¹Department of Geosciences, University of Oslo, Oslo, Norway

Key Points:

- Ice-nucleating particles (INPs) control ice formation in high-latitude clouds.
- Sea ice and snow inhibit the local emission of INPs, which directly influences cloud phase in the Arctic and Southern Ocean.
- This has implications for the predicted negative cloud phase feedback with future warming and the associated sea ice and snow cover loss.

*Both authors contributed equally to this work.

Corresponding author: Tim Carlsen and Robert O. David, tim.carlsen@geo.uio.no,
r.o.david@geo.uio.no

Abstract

Mixed-phase clouds (MPCs), which consist of both supercooled cloud droplets and ice crystals, play an important role in the Earth's radiative energy budget and hydrological cycle. In particular, the fraction of ice crystals in MPCs determines their radiative effects, precipitation formation and lifetime. In order for ice crystals to form in MPCs, ice-nucleating particles (INPs) are required. However, a large-scale relationship between INPs and ice initiation in clouds has yet to be observed. By analyzing satellite observations of the typical transition temperature (T^*) where MPCs become more frequent than liquid clouds, we constrain the importance of INPs in MPC formation. We find that over the Arctic and Southern Ocean, snow and sea ice cover significantly reduces T^* . This indicates that the availability of INPs is essential in controlling cloud phase evolution and that local sources of INPs in the high-latitudes play a key role in the formation of MPCs.

Plain Language Summary

Mixed-phase clouds (MPCs), which consist of both liquid droplets and ice crystals, play an important role for the Earth's climate system. For example, the number of ice crystals in MPCs determines how much sunlight is reflected by the cloud and how efficiently the cloud can form precipitation. The formation of ice crystals in MPCs requires a special subset of aerosol particles called ice-nucleating particles (INPs). INPs are required for liquid cloud droplets to freeze at temperatures warmer than -36°C . However, a large-scale relationship between INPs and ice formation in clouds has yet to be observed. Using satellite observations, we determine the transition temperature (T^*) where MPCs become more frequent than liquid clouds and find that T^* is strongly dependent on snow and sea ice cover over the Arctic and Southern Ocean. This indicates that sea ice and snow cover act as a lid that inhibits the emission of INPs from the ocean. In a warming world with retreating sea ice and snow cover, our results suggest that clouds in these regions will contain ice crystal at warmer temperatures than previously estimated and thus, have potential implications for future warming predictions.

1 Introduction

The amount of liquid and ice within MPCs influences precipitation formation, cloud lifetime, and electrification (Cantrell & Heymsfield, 2005). Simultaneously, the thermodynamic phase composition controls the radiative properties of MPCs due to the different scattering properties between liquid water and ice. In a warming climate, MPCs are believed to transition towards a state with more liquid water and a higher albedo, which limits future warming (Bjorndal et al., 2020; Zelinka et al., 2020). This cloud phase feedback makes the accurate representation of ice crystal concentrations in MPCs in Earth System Models (ESMs) essential for correctly predicting the future climate (Tan et al., 2016; Forster et al., 2021). But what controls the formation of ice and the thermodynamic phase composition in MPCs?

The importance of INPs for forming ice in MPCs is undisputed. Laboratory experiments show that pure water does not freeze without the presence of an INP until it is supercooled to around -36°C . Therefore, field measurements including precipitation sampling (Vali, 1971; Petters & Wright, 2015), airborne (Borys, 1989; Rogers et al., 2001; Pratt et al., 2009; DeMott et al., 2010), ship (Wilson et al., 2015; Welti et al., 2020), and mountaintop measurements (Lacher et al., 2017) have been conducted to investigate the abundance of INPs, globally. These studies have found that INP concentrations can vary by several orders of magnitude at a given temperature. This variability is partially explained by the location and type of aerosol acting as INPs (Kanji et al., 2017). Close to the Earth's major deserts, dust is the primary source of INPs, especially at temperatures below -15°C (Atkinson et al., 2013; Murray et al., 2012; Boose et al., 2016). Meanwhile,

in more remote regions and at higher temperatures, biological sources such as sea spray aerosol are believed to be the most important source of INPs (Burrows et al., 2013; Schnell & Vali, 1975; Wilson et al., 2015; C. S. McCluskey et al., 2018; Irish et al., 2019).

Based on the fundamental importance of INPs for ice crystal formation in MPCs, INP parametrizations have been developed to account for different aerosol species and the observed variability from field and laboratory studies. When implemented into ESMs, different INP parametrizations can have profound effects on both MPC optical properties and lifetimes. However, when in situ ice crystal number concentrations are compared with INP concentrations, they seldomly agree (Mignani et al., 2019) and ice crystal concentrations often exceed INP concentrations by several orders of magnitude (Ladino et al., 2017; Ramelli et al., 2021; Rangno & Hobbs, 2001). This would suggest that INPs are not as important for ice crystal formation in MPCs as laboratory studies indicate. The main explanation for this discrepancy is secondary ice production (SIP) (Korolev & Leisner, 2020; Hallett & Mossop, 1974), which has been shown to rapidly increase the concentration of ice crystals in MPCs through what has been described as a cascading process. Nevertheless, the occurrence and efficiency of secondary ice processes is still an area of open research.

Another and larger scale approach to assess the influence of INPs on MPCs has been through the so-called supercooled liquid fraction (SLF, ratio of supercooled liquid to ice). The SLF and ambient aerosol concentration (a proxy for INPs) comparisons show that there is a correlation, but a weak dependence between dust aerosols and the SLF of MPCs at a given temperature (Choi et al., 2010; Tan et al., 2014). However, the SLF is prone to the influence of dynamics (vertical velocities), the Wegener-Bergeron-Findeisen process (Korolev, 2007), and secondary ice processes, thereby masking the importance of INPs for the distribution of the cloud phase.

Therefore, with the exception of laboratory and modeling studies, direct evidence of the importance of INPs on MPC formation and subsequent thermodynamic phase composition has yet to be observed or quantified. Here we show that by using the transition temperature from supercooled liquid clouds to MPCs, as observed by satellites, the influence of INPs on the thermodynamic phase composition in MPCs can be disentangled. In particular, we focus this analysis on the high-latitudes, where MPCs are abundant (Korolev et al., 2017). Additionally, field studies indicate that local INP emissions have a strong seasonal dependence in the Arctic (Wex et al., 2019; Tobo et al., 2019), providing a unique opportunity to analyse the influence of differing INP concentrations on MPCs. We find that this transition temperature is significantly suppressed over sea ice and snow, confirming that INPs play a critical role in the evolution of cloud phase and that the INPs in this region are primarily of a local nature.

2 Materials and Methods

Here we use satellite observations from CloudSat and the Cloud-Aerosol Lidar and Infrared Pathfinder Satellite Observation (CALIPSO, Stephens et al., 2002; Winker et al., 2010) to discriminate between single-layer liquid only (LO) and liquid-topped MPCs (LTMPs) and combine them with cloud top temperatures (CTTs) from atmospheric reanalysis data to characterize the occurrence of both cloud types as a function of CTT (see Figs. 1A and B). The warmest CTT when LTMPs become more frequent than LO clouds, is hereafter referred to as T^* (see Fig. 1C). We perform this analysis on a $5^\circ \times 5^\circ$ grid (see Fig. 1D) for each season over 9 years (2006-2017). In this section, the calculation of T^* , its significance, and the averaging procedure are described together with the processing of the sea ice data used in the interpretation of the results.

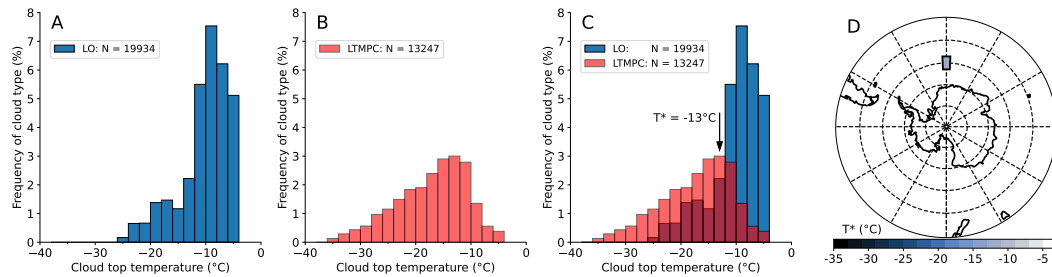


Figure 1. Frequency of cloud types (in %) with respect to cloud top temperature (bin width: 2°C) for the 5°x5° grid cell centered at 60°S and 0°E combining 9 austral summer seasons (DJF, 2006-2009 and 2012-2016). (A) for liquid-only clouds, (B) for liquid-top mixed-phase clouds, (C) The combination of LO and LTMPC frequency distributions yields an exemplary T^* of -13°,C.

2.1 Satellite data and definition of cloud regimes

For the discrimination between LO clouds and LTMPCs, we use the data product 2B-CLDCLASS-LIDAR (Sassen et al., 2008), which combines observations from the cloud profiling radar (CPR) on CloudSat (Stephens et al., 2002) and the Cloud-Aerosol Lidar with Orthogonal Polarization (CALIOP) (Winker et al., 2007) on CALIPSO (Winker et al., 2010). The 2B-CLDCLASS-LIDAR product utilizes the different sensitivities of the radar and lidar to liquid droplets and ice crystals to determine the phase of a cloud layer. The logics of the phase determination algorithm are based on a temperature dependent radar reflectivity threshold (Zhang et al., 2010), the integrated attenuated lidar backscattering coefficient, and cloud base and top temperatures from atmospheric reanalysis (Wang, 2019). This way, each individual cloud layer of the CPR profile gets assigned a phase (variable `CloudPhase`: 'ice', 'mixed', or 'water'). Here we restrict our analysis to single-layer clouds. The cloud phase information comes with a confidence level assigned to the cloud phase (variable `CloudPhaseConfidenceLevel`). The confidence value generally ranges from zero to 10, where 10 indicates the highest confidence level. While it is not recommended to use data with a confidence level of five or lower, we further restrict our analysis to cloud phase confidence levels of seven or higher. For each cloudy profile, we retrieve the cloud top temperature (CTT) from the ECMWF-AUX dataset that contains ancillary European Centre for Medium-Range Weather Forecast (ECMWF) state variable data interpolated to each CPR vertical bin. For the definition of the different cloud types, we include observations with CTTs below 270 K to stay away from the temperature limits of the phase determination algorithm. We define LO clouds and MPCs based on the `CloudPhase` variable of 'water' or 'mixed', respectively. For the definition of LTMPCs, we further use the `Water_layer_top` variable from the 2B-CLDCLASS-LIDAR product, which indicates the location of a possible water layer in MPCs. We define LTMPCs as all MPCs where the `Water_layer_top` is within 3 vertical radar bins (90 m) of the cloud top height (variable `CloudLayerTop`). The CTT of all LO and LTMPC are combined into 5°x5° grid cells over the entire globe. Then the CTTs of the LO and LTMPCs are binned into 2°C temperature bins by season for the years 2006 to 2017.

For each 5°x5° grid cell, the LO and LTMPC observations are normalized by the total number of single-layer observations (LO, MPCs, ice-only) in the given cell. Finally, T^* is then defined as the warmest CTT bin, where LTMPCs are more frequent than LO clouds and where at least 10 LTMPCs were observed within that given season summed over the nine year period.

2.2 Significance of T^*

To test the robustness and significance of T^* , its calculation is repeated 100 times using random sampling with replacement (bootstrapping) of the original observations of both LO and LTMPs for each grid cell and each season. The significance of T^* is estimated based on the distribution of the T^* values from the bootstrapped calculations by calculating the standard error (SE) from the standard deviation σ of the bootstrapped T^* and the number of bootstrapped T^* values (100):

$$SE = \frac{\sigma}{\sqrt{100}} \quad (1)$$

From the SE, the 99 % confidence interval (CI) can be calculated as:

$$CI = 2.58 \cdot SE \quad (2)$$

Grid cells are classified as insignificant if the CI is larger than 0.5°C (corresponding to a T^* confined to about 1 bin during bootstrapping) and are excluded from the analysis. Most grid cells analysed within this study show very robust T^* values (see Fig. S1).

For the difference in T^* (Summer - Winter) in Fig. 2C and F, the grid cells where the sum of the summer and winter CIs is larger than the absolute value of the T^* difference (min/max error propagation) are treated as insignificant.

2.3 Sea ice data

The sea ice concentration data is from the Institute of Environmental Physics (IUP), University of Bremen, based on the ARTIST Sea Ice (ASI) algorithm (Spren et al., 2008). The ASI retrieval is applied to microwave radiometer data of the AMSR-E (Advanced Microwave Scanning Radiometer for EOS) on the Aqua satellite and AMSR2 (Advanced Microwave Scanning Radiometer 2) on GCOM-W1 sensors, which were reprocessed in 2018 for both platforms with the same parameters. The sea ice edge as visible in Fig. 2 is calculated using the following steps: (1) Retrieval of the dates for the Arctic/Antarctic sea ice maximum/minimum for each year (Grosfeld et al., 2016) and calculation of the multi-year average of the sea ice maxima/minima from these days. If the maximum/minimum occurred in March/September, we used the last day of the respective season (February/August) in the calculation. (2) The sea ice edge is defined where the sea ice concentration is at least 15 %. (3) Re-gridding of the sea ice data on a regular $0.25^\circ \times 0.25^\circ$ grid using bilinear interpolation.

2.4 Averaging of T^*

We perform area-weighted averaging of T^* for the different regions and seasons based on the sea ice concentrations and land/ocean masks (from ASI data set) that we re-gridded on the $5^\circ \times 5^\circ$ grid of T^* using bilinear interpolation. Further, grid cells with insignificant T^* values are excluded from the averaging. The resulting masks used for the calculation of the average T^* values in Table 1 are displayed in Figure S2.

3 Results and discussion

T^* is based on the underlying principle that as the CTT of LO clouds cool, the initiation of ice becomes more likely as a larger fraction of aerosols can act as INPs (Fletcher, 1962; Meyers et al., 1992) and therefore, the probability of observing LTMPs increases. As shown by the exemplary histograms in Fig. 1, the observed frequency of LTMPs increases at colder temperatures, as expected, and exceeds that of LO clouds at -13°C . Therefore, in this example the T^* of -13°C represents the typical temperature at which INPs act to alter the cloud phase for this region.

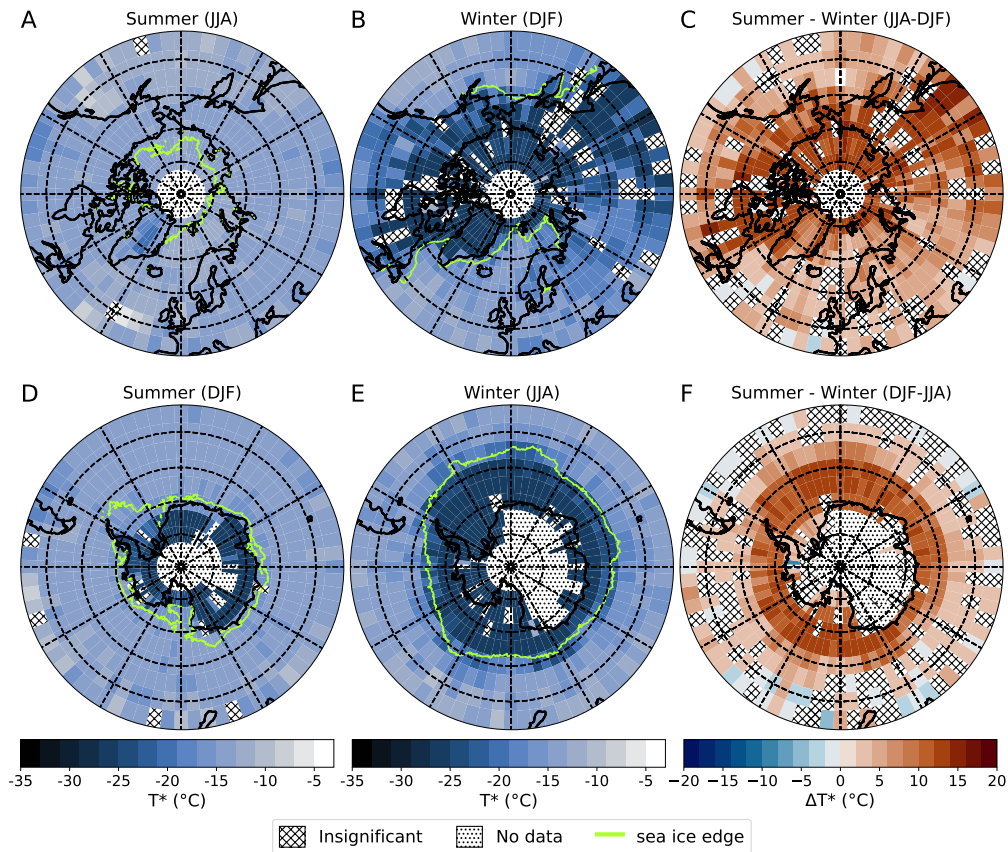


Figure 2. Seasonal T^* over the Arctic and the Southern Ocean based on observations between 2006-2017. Grid cells where T^* calculations are insignificant (on a 99 % confidence level) are hatched, while dotted areas have no data. The green line shows the average minimum/maximum sea ice edge between 2006-2017, defined as the 15% sea ice concentration line for the given season. Arctic T^* during Summer (JJA), Winter T^* (DJF) and the difference between Summer and Winter (Summer minus Winter) are shown in panel A,B, and C, respectively. Similarly, the Southern Ocean T^* during Austral Summer (DJF), Winter (JJA) and the difference between Summer and Winter (Summer minus Winter) are shown in panel D,E and F, respectively.

When calculating T^* over the Arctic as a function of sea and land mask (see Tab. 1), we find that during the summer time (JJA), T^* is -13°C over the Ocean and -14°C over land (Fig. 2A). At these temperature, biological INPs are expected to be dominant (Kanji et al., 2017) and indeed field studies have shown that INPs are primarily biological during the Arctic summer (Tobo et al., 2019; Creamean et al., 2019). T^* is homogeneous over both the land and the ocean and this suggests that the abundance of INPs and their efficiency is rather similar throughout the region. The only exception is over the Greenland ice sheet (lower T^* values, see Fig. 2A) where due to its high altitude and frequently cold temperatures, INPs are expected to be washed out during transport to this area (Stopelli et al., 2015) or relatively INP depleted air from the free troposphere (Lacher et al., 2018) descends over the ice sheet (Guy et al., 2021). Consistently, field measurements have shown that INP concentrations are lower over the Greenland ice sheet than elsewhere during the Arctic summertime (Wex et al., 2019).

Table 1. Area-weighted averages of significant T^* (in $^{\circ}\text{C}$) for different regions and seasons. The masks used for averaging are displayed in Fig. S2.

Arctic	ocean	land	sea ice
Summer (JJA)	-13	-14	-
Winter (DJF)	-16	-23	-24
Antarctica	ocean	land	sea ice
Summer (DJF)	-15	-	-
Winter (JJA)	-17	-	-27

In contrast, during the winter months (DJF) the T^* over the sea ice region (green line in Fig. 2) drops to -24°C , while over open ocean it slightly decreases to -16°C (Fig. 2B, compare Tab. 1). Similarly, during the winter months snow cover reduces T^* to -23°C over land. Thus, the largest seasonal differences in T^* are observed in regions covered by snow and sea ice during the winter (Fig. 2C). Previous ship (Bigg, 1996; Bigg & Leck, 2001) and coastal (Creamean et al., 2018) measurements also observed a dependence of the INP concentration on the extent of snow and sea ice coverage, with a decrease and increase in INP concentration during the Fall freeze up and Spring thaw, respectively. A reduction in wintertime INP concentration was also observed at an inland Arctic location in Alaska (Borys, 1983) and a Boreal Forest in Finland (Schneider et al., 2021). Similarly, Wex et al. (2019) observed an increase in INPs during the snow-free summer months and a decrease during the winter months at four different measurement locations in the Arctic. Their back trajectory analysis showed that the highest INP concentrations were associated with air mass interaction with snow-free terrain and open water, while the lowest concentrations came from the sea ice and snow.

Airborne Arctic INP measurements (Borys, 1989; Hartmann et al., 2020) also observed a decrease in INP concentration over sea ice and snow cover. The only exception was over open leads in the sea ice (Rogers et al., 2001; Hartmann et al., 2020; Curry et al., 2000), which further indicates that sea ice inhibits the emissions of INPs. This lack of available biological INPs has also been used to explain the lower temperatures required to observe MPCs in the Arctic relative to the midlatitudes and tropics (Costa et al., 2017). Furthermore, Griesche et al. (2021) observed a decrease in the frequency of ice containing clouds when they were decoupled from the ocean surface, also indicating that marine INPs are essential for ice formation in Arctic clouds.

These studies are in agreement with our findings, that sea ice and snow cover significantly reduce T^* . Thus, the combination of previous INP studies with the T^* metric presented here demonstrates the large-scale influence INPs have on the formation of MPCs in the Arctic.

When calculating T^* over the Southern Ocean and separating by season (Figs. 2D-F, Tab. 1), it is apparent that T^* is -15°C during the Austral summer (DJF) and homogeneous over the entire region. This is consistent with summertime ship measurements conducted in the Southern Ocean, where INPs were typically observed at temperatures above -14°C (Welti et al., 2020; C. McCluskey et al., 2018) and their concentration only varied by about one order of magnitude at -15°C (Welti et al., 2020). When comparing to the Arctic, the summertime T^* in the Southern Ocean is about 2°C cooler. This may in part be due to higher biological activity in the Arctic Ocean (McCluskey et al., 2019; Irish et al., 2017) and a larger land area where glacial out wash can be emitted and act as a local episodic INP source (Sanchez-Marroquin et al., 2020; Tobo et al., 2019; Rinaldi et al., 2021). Meanwhile, during the winter (JJA), a similar relationship between

sea ice coverage and T^* emerges (Fig. 2E). The T^* over the sea ice region drops to -27°C , while over open ocean regions the T^* slightly decreases to -17°C . This indicates that the sea ice acts to inhibit the emission of INPs and directly impacts cloud phase over the Southern Ocean as well. It is well known that the ocean is an important source of INPs in the Southern Ocean (Schnell, 1977; Burrows et al., 2013), which is far from the Earth's deserts (DeMott et al., 2016; C. McCluskey et al., 2018). Indeed, INP observations from South Pole were significantly lower than at a coastal site (Belosi et al., 2014) and increased when airmass back trajectories originated from the coast (Ardon-Dryer et al., 2011). Modelling studies have shown that replacing dust-based with marine-based INP parametrizations greatly improves the representation of clouds over the Southern Ocean (Vergara-Temprado et al., 2018; Frey & Kay, 2018). This further provides evidence that the Southern Ocean is the primary source of INPs over this region and when it is covered with sea ice, fewer INPs are emitted. Therefore, our results indicate that the decrease in T^* over the sea ice is a result of the sea ice acting as a lid that inhibits the emission of INPs from the Southern Ocean and, in turn, hinders the initiation of MPCs in this region.

Previous remote sensing observations of cloud phase over the Southern Ocean have also observed a spatial pattern in the occurrence of MPCs (e.g., Mace et al., 2020, 2021) with a maximum in the vicinity of the so-called Antarctic Polar Front (APF, Freeman & Lovenduski, 2016). Mace et al. (2021) attributed this relationship to potentially enhanced vertical updrafts in convective clouds over the APF due to warmer sea surface temperatures, which would loft ice crystals from lower layers of clouds to their top where a lidar-depolarization based cloud classification algorithm (Mace et al., 2020) would classify them as mixed-phase. Additionally, they highlight that these enhanced updrafts would act as a production zone for larger cloud droplets, which have been shown to be more efficient for SIP (Lauber et al., 2018; Keinert et al., 2020). Although we cannot rule out the importance of SIP on the classification of a cloud as LTMPC, through the combined use of lidar and radar observations in the 2B-CLDCLASS-LIDAR product we can reduce the importance of ice crystals being lofted to cloud top for the classification of LTMPCs. Regardless of the importance of SIP in producing ice in LTMPCs, primary ice formed on INPs is still required and thus, T^* is representative of when INPs are responsible for controlling the cloud phase over the SO. Furthermore, when comparing T^* values with the location of the APF in the summertime (see Fig. 3 in Freeman & Lovenduski, 2016) there is no clear dependence, indicating that the observed seasonal variability in T^* is associated with the sea ice extent and its ability to inhibit INP emissions.

With this in mind, it is important to note that there are well-documented differences in high-latitude clouds over the open ocean and sea ice due to differences in surface fluxes (e.g. heat and moisture) and thermodynamic structure (Palm et al., 2010; Eirund et al., 2019; Sotiropoulou et al., 2016; Young et al., 2017). However, to our knowledge these differences would not lead to LO clouds occurring more frequently at colder temperatures over sea ice than over open water as we observe. Furthermore, when comparing the cloud top heights and occurrence of LO and LTMPCs over the Southern Ocean (see Fig. S3), we find that they overlap and occur at the same heights in the troposphere, regardless of whether they form over open ocean or sea ice. Therefore, the observed variability in T^* can only be explained by the variability in the efficiency and concentration of INPs present during the onset of ice formation and MPC initiation.

4 Atmospheric implications

The apparent relationship between the suppressed T^* and sea ice and snow cover (Fig. 2), which is well documented as a region with reduced INP concentrations (Wex et al., 2019; Bigg & Leck, 2001; Creamean et al., 2019), indicates that INPs play a critical role in the initiation of MPCs. Furthermore, this relationship provides additional evidence that INPs in the high-latitudes are primarily of a local origin. Ultimately, through the use of T^* , we highlight the global relevance of INPs on MPC formation, confirming

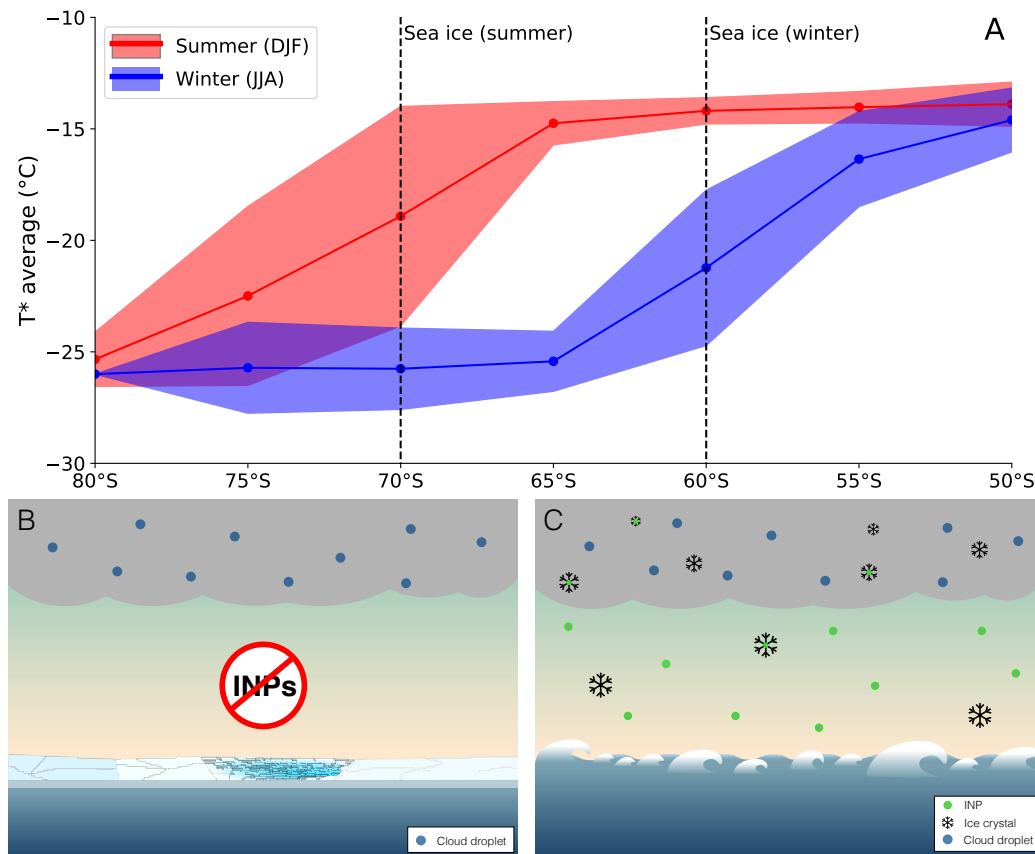


Figure 3. (A) Latitudinal average (line) and standard deviation (fill) of T^* during Austral summer (red) and winter (blue) over the Southern Ocean as a northward cross section from 80°S to 50°S. (B-C) Conceptual overview of how sea ice cover influences INP sources and, consequently, ice formation in MPCs.

laboratory studies dating back to the 1940s (Vonnegut, 1947) that showed the importance of INPs for MPC formation.

Based on these findings, we conclude that differing INP parametrizations are required over ice/snow-covered and ice/snow-free portions of the high-latitudes to account for the observed seasonal variations in the MPC transition temperature, T^* . This is especially important for future climate projections, where in a warming climate, sea ice and snow cover are projected to decrease (Fox-Kemper et al., 2021) and therefore, although temperatures will rise, INPs may become more abundant due to newly available source regions (i.e. ice and snow free areas).

An increase in the abundance of high-latitude INPs could have profound effects on the cloud-phase feedback (Murray et al., 2021; Prenni et al., 2007), which has so far been projected to limit warming over the Southern Ocean (Forster et al., 2021; Zelinka et al., 2020; Bjordal et al., 2020; Tan et al., 2016). The warming-induced INP increase could weaken, or even reverse, the projected increase in LO clouds with warming. This would have major implications for both the magnitude and sign of the Southern Ocean cloud feedback, thus shaping the climate evolution of the region itself and ultimately, the future climate of the entire planet. Figure 3 shows the T^* averaged by latitude over the Southern Ocean. The stark contrast in T^* over sea ice and open ocean indicates that in a warming world with sea ice retreat, T^* over formerly ice covered regions will increase

to -15 °C. As the ice covered regions currently have a T^* of approximately -25 °C, this would suggest that a warming of 10 °C would be required to significantly offset the formation of MPCs over future ice free regions of the Southern Ocean. Therefore, without a detailed quantification of the seasonal nature of INPs in the high-latitudes and subsequent inclusion in ESMs, the influence of the negative cloud phase-feedback on buffering future warming will remain uncertain.

5 Open Research

The standard CloudSat (Stephens et al., 2002) and CALIPSO (Winker et al., 2010) data products (version R05) used in this study (2B-CLDCLASS-LIDAR, ECMWF-AUX) were downloaded from the CloudSat Data Processing Center's (at Cooperative Institute for Research in the Atmosphere, Colorado State University, Fort Collins) website (<http://www.cloudsat.cira.colostate.edu>).

The sea ice concentration data is from the Institute of Environmental Physics (IUP), University of Bremen, based on the ARTIST Sea Ice (ASI) algorithm (Spreen et al., 2008). The daily data sets (Melsheimer & Spreen, 2020b, 2020a, 2019b, 2019a) were downloaded for the years 2006-2017 from the data publisher PANGAEA. The dates for the Arctic and Antarctic sea ice maximum/minimum for each year were retrieved from <https://www.meereisportal.de> (Grosfeld et al., 2016).

The code used to analyse the satellite data will be made available on a public GitHub repository pending final publication of this manuscript.

Acknowledgments

We gratefully acknowledge the funding by the European Research Council (ERC) through Grant StG758005. ROD would also like to acknowledge EEARO-NO-2019-0423/IceSafari, contract no. 31/2020, under the NO grants 2014–2021 of EEA Grants/Norway Grants for financial support. We would also like to thank Trude Storelvmo for her support and valuable insight throughout the development of this project and during the writing of this manuscript. Sea ice concentration data from 2006 to 2017 were obtained from <https://www.meereisportal.de> (grant: REKLIM-2013-04). Lastly, we would like to acknowledge the USIT statistikk service at University of Oslo and, in particular, Sahar Hassani for contributing her statistical expertise to this analysis.

References

- Ardon-Dryer, K., Levin, Z., & Lawson, R. P. (2011). Characteristics of immersion freezing nuclei at the south pole station in antarctica. *Atmospheric Chemistry and Physics*, 11(8), 4015–4024. Retrieved from <https://acp.copernicus.org/articles/11/4015/2011/> doi: 10.5194/acp-11-4015-2011
- Atkinson, J., Murray, B., Woodhouse, M., Whale, T., Baustian, K., Carslaw, K., ... Malkin, T. (2013, 06). The importance of feldspar for ice nucleation by mineral dust in mixed-phase clouds. *Nature*, 498. doi: 10.1038/nature12278
- Belosi, F., Santachiara, G., & Prodi, F. (2014). Ice-forming nuclei in antarctica: New and past measurements. *Atmospheric Research*, 145-146, 105-111. Retrieved from <https://www.sciencedirect.com/science/article/pii/S0169809514001549> doi: <https://doi.org/10.1016/j.atmosres.2014.03.030>
- Bigg, E. K. (1996). Ice forming nuclei in the high arctic. *Tellus B: Chemical and Physical Meteorology*, 48(2), 223-233. Retrieved from <https://doi.org/10.3402/tellusb.v48i2.15888> doi: 10.3402/tellusb.v48i2.15888
- Bigg, E. K., & Leck, C. (2001). Properties of the aerosol over the central arctic ocean. *Journal of Geophysical Research: Atmospheres*, 106(D23), 32101-32109. Retrieved from <https://agupubs.onlinelibrary.wiley.com/doi/abs/>

- 10.1029/1999JD901136 doi: <https://doi.org/10.1029/1999JD901136>
- Bjorndal, J., Storelvmo, T., Alterskjær, K., & Carlsen, T. (2020). Equilibrium climate sensitivity above 5°C plausible due to state-dependent cloud feedback. *Nature Geoscience*, 13, 718 - 721.
- Boose, Y., Sierau, B., García, M. I., Rodríguez, S., Alastuey, A., Linke, C., ... Lohmann, U. (2016). Ice nucleating particles in the saharan air layer. *Atmospheric Chemistry and Physics*, 16(14), 9067–9087. Retrieved from <https://acp.copernicus.org/articles/16/9067/2016/> doi: 10.5194/acp-16-9067-2016
- Borys, R. D. (1983). *The effects of long range transport of air pollutants on arctic cloud active aerosol* (The effects of long range transport of air pollutants on Arctic cloud active aerosol, Atmos. Sci. (paper no. 367)). Dept. Atmos. Sci. Colorado State Univ., Ft. Collins, USA.
- Borys, R. D. (1989). Studies of ice nucleation by arctic aerosol on agasp-ii. *Journal of Atmospheric Chemistry*, 9, 169-185.
- Burrows, S. M., Hoose, C., Pöschl, U., & Lawrence, M. G. (2013). Ice nuclei in marine air: biogenic particles or dust? *Atmospheric Chemistry and Physics*, 13(1), 245–267. Retrieved from <https://acp.copernicus.org/articles/13/245/2013/> doi: 10.5194/acp-13-245-2013
- Cantrell, W., & Heymsfield, A. (2005). Production of ice in tropospheric clouds: A review. *Bulletin of the American Meteorological Society*, 86(6), 795 - 808. Retrieved from <https://journals.ametsoc.org/view/journals/bams/86/6/bams-86-6-795.xml> doi: 10.1175/BAMS-86-6-795
- Choi, Y.-S., Lindzen, R. S., Ho, C.-H., & Kim, J. (2010). Space observations of cold-cloud phase change. *Proceedings of the National Academy of Sciences*, 107(25), 11211–11216. Retrieved from <https://www.pnas.org/content/107/25/11211> doi: 10.1073/pnas.1006241107
- Costa, A., Meyer, J., Afchine, A., Luebke, A., Günther, G., Dorsey, J. R., ... Krämer, M. (2017). Classification of arctic, midlatitude and tropical clouds in the mixed-phase temperature regime. *Atmospheric Chemistry and Physics*, 17(19), 12219–12238. Retrieved from <https://acp.copernicus.org/articles/17/12219/2017/> doi: 10.5194/acp-17-12219-2017
- Creamean, J. M., Cross, J. N., Pickart, R., McRaven, L., Lin, P., Pacini, A., ... DeMott, P. J. (2019). Ice nucleating particles carried from below a phytoplankton bloom to the arctic atmosphere. *Geophysical Research Letters*, 46(14), 8572-8581. Retrieved from <https://agupubs.onlinelibrary.wiley.com/doi/abs/10.1029/2019GL083039> doi: <https://doi.org/10.1029/2019GL083039>
- Creamean, J. M., Kirpes, R. M., Pratt, K. A., Spada, N. J., Maahn, M., de Boer, G., ... China, S. (2018). Marine and terrestrial influences on ice nucleating particles during continuous springtime measurements in an arctic oilfield location. *Atmospheric Chemistry and Physics*, 18(24), 18023–18042. Retrieved from <https://acp.copernicus.org/articles/18/18023/2018/> doi: 10.5194/acp-18-18023-2018
- Curry, J. A., Hobbs, P. V., King, M. D., Randall, D. A., Minnis, P., Isaac, G. A., ... Wylie, D. (2000). Fire arctic clouds experiment. *Bulletin of the American Meteorological Society*, 81(1), 5 - 30. Retrieved from https://journals.ametsoc.org/view/journals/bams/81/1/1520-0477_2000_081_0005_face_2_3_co_2.xml doi: 10.1175/1520-0477(2000)081<0005:FACE>2.3.CO;2
- DeMott, P. J., Hill, T. C. J., McCluskey, C. S., Prather, K. A., Collins, D. B., Sullivan, R. C., ... Franc, G. D. (2016). Sea spray aerosol as a unique source of ice nucleating particles. *Proceedings of the National Academy of Sciences*, 113(21), 5797–5803. Retrieved from <https://www.pnas.org/content/113/21/5797> doi: 10.1073/pnas.1514034112
- DeMott, P. J., Prenni, A. J., Liu, X., Kreidenweis, S. M., Petters, M. D., Twohy, C. H., ... Rogers, D. C. (2010). Predicting global atmospheric ice nuclei dis-

- tributions and their impacts on climate. *Proceedings of the National Academy of Sciences*, 107(25), 11217–11222. Retrieved from <https://www.pnas.org/content/107/25/11217> doi: 10.1073/pnas.0910818107
- Eirund, G. K., Possner, A., & Lohmann, U. (2019). Response of arctic mixed-phase clouds to aerosol perturbations under different surface forcings. *Atmospheric Chemistry and Physics*, 19(15), 9847–9864. Retrieved from <https://acp.copernicus.org/articles/19/9847/2019/> doi: 10.5194/acp-19-9847-2019
- Fletcher, N. H. (1962). *The physics of rainclouds*. Cambridge University Press.
- Forster, P., Storelvmo, T., Armour, K., Collins, W., Dufresne, J.-L., Frame, D., ... Zhang, X. (2021). The Earth's energy budget, climate feedbacks, and climate sensitivity. In V. Masson-Delmotte et al. (Eds.), *Climate Change 2021: The Physical Science Basis. Contribution of Working Group I to the Sixth Assessment Report of the Intergovernmental Panel on Climate Change*. Cambridge University Press.
- Fox-Kemper, B., Hewitt, H. T., Xiao, C., Aalgeirsdóttir, G., Drijfhout, S. S., Edwards, T. L., ... Yu, Y. (2021). Ocean, cryosphere, and sea level change. In V. Masson-Delmotte et al. (Eds.), *Climate Change 2021: The Physical Science Basis. Contribution of Working Group I to the Sixth Assessment Report of the Intergovernmental Panel on Climate Change*. Cambridge University Press.
- Freeman, N. M., & Lovenduski, N. S. (2016). Mapping the antarctic polar front: weekly realizations from 2002 to 2014. *Earth System Science Data*, 8(1), 191–198. Retrieved from <https://essd.copernicus.org/articles/8/191/2016/> doi: 10.5194/essd-8-191-2016
- Frey, W. R., & Kay, J. E. (2018). The influence of extratropical cloud phase and amount feedbacks on climate sensitivity. *Climate Dynamics*, 50, 3097–3116.
- Griesche, H. J., Ohneiser, K., Seifert, P., Radenz, M., Engelmann, R., & Ansmann, A. (2021). Contrasting ice formation in arctic clouds: surface-coupled vs. surface-decoupled clouds. *Atmospheric Chemistry and Physics*, 21(13), 10357–10374. Retrieved from <https://acp.copernicus.org/articles/21/10357/2021/> doi: 10.5194/acp-21-10357-2021
- Grosfeld, K., Treffeisen, R., Asseng, J., Bartsch, A., Bräuer, B., Fritzsche, B., ... Weigelt, M. (2016, June). *Online sea-ice knowledge and data platform <www.meereisportal.de>* (Vol. 85) (No. 2). Bremerhaven: Alfred Wegener Institute for Polar and Marine Research & German Society of Polar Research. doi: 10.2312/polfor.2016.011
- Guy, H., Brooks, I. M., Carslaw, K. S., Murray, B. J., Walden, V. P., Shupe, M. D., ... Neely III, R. R. (2021). Controls on surface aerosol particle number concentrations and aerosol-limited cloud regimes over the central greenland ice sheet. *Atmospheric Chemistry and Physics*, 21(19), 15351–15374. Retrieved from <https://acp.copernicus.org/articles/21/15351/2021/> doi: 10.5194/acp-21-15351-2021
- Hallett, J., & Mossop, S. C. (1974). Production of secondary ice particles during the riming process. *Nature*, 249(5452), 26–28. Retrieved from <https://app.dimensions.ai/details/publication/pub.1047745896> doi: 10.1038/249026a0
- Hartmann, M., Adachi, K., Eppers, O., Haas, C., Herber, A., Holzinger, R., ... Stratmann, F. (2020). Wintertime airborne measurements of ice nucleating particles in the high arctic: A hint to a marine, biogenic source for ice nucleating particles. *Geophysical Research Letters*, 47(13), e2020GL087770. Retrieved from <https://agupubs.onlinelibrary.wiley.com/doi/abs/10.1029/2020GL087770> (e2020GL087770 10.1029/2020GL087770) doi: <https://doi.org/10.1029/2020GL087770>
- Irish, V. E., Elizondo, P., Chen, J., Chou, C., Charette, J., Lizotte, M., ... Bertram, A. K. (2017). Ice-nucleating particles in canadian arctic sea-surface microlayer

- 466 and bulk seawater. *Atmospheric Chemistry and Physics*, 17(17), 10583–10595.
467 Retrieved from <https://acp.copernicus.org/articles/17/10583/2017/>
468 doi: 10.5194/acp-17-10583-2017
- 469 Irish, V. E., Hanna, S. J., Xi, Y., Boyer, M., Polishchuk, E., Ahmed, M., ...
470 Bertram, A. K. (2019). Revisiting properties and concentrations of ice-
471 nucleating particles in the sea surface microlayer and bulk seawater in the
472 canadian arctic during summer. *Atmospheric Chemistry and Physics*, 19(11),
473 7775–7787. Retrieved from [https://acp.copernicus.org/articles/19/](https://acp.copernicus.org/articles/19/7775/2019/)
474 7775/2019/ doi: 10.5194/acp-19-7775-2019
- 475 Kanji, Z. A., Ladino, L. A., Wex, H., Boose, Y., Burkert-Kohn, M., Cziczo, D. J., &
476 Krämer, M. (2017). Overview of ice nucleating particles. *Meteorological Mono-*
477 *graphs*, 58, 1.1 - 1.33. Retrieved from [https://journals.ametsoc.org/](https://journals.ametsoc.org/view/journals/amsm/58/1/amsmonographs-d-16-0006.1.xml)
478 [view/journals/amsm/58/1/amsmonographs-d-16-0006.1.xml](https://journals/amsm/58/1/amsmonographs-d-16-0006.1.xml) doi:
479 10.1175/AMSMONOGRAPHS-D-16-0006.1
- 480 Keinert, A., Spannagel, D., Leisner, T., & Kiselev, A. (2020). Secondary ice
481 production upon freezing of freely falling drizzle droplets. *Journal of*
482 *the Atmospheric Sciences*, 77(8), 2959 - 2967. Retrieved from [https://](https://journals.ametsoc.org/view/journals/atsc/77/8/jasD200081.xml)
483 journals.ametsoc.org/view/journals/atsc/77/8/jasD200081.xml doi:
484 10.1175/JAS-D-20-0081.1
- 485 Korolev, A. (2007). Limitations of the wegener–bergeron–findeisen mechanism in
486 the evolution of mixed-phase clouds. *Journal of the Atmospheric Sciences*,
487 64(9), 3372 - 3375. Retrieved from [https://journals.ametsoc.org/view/](https://journals.ametsoc.org/view/journals/atsc/64/9/jas4035.1.xml)
488 journals/atsc/64/9/jas4035.1.xml doi: 10.1175/JAS4035.1
- 489 Korolev, A., & Leisner, T. (2020). Review of experimental studies of secondary ice
490 production. *Atmospheric Chemistry and Physics*, 20(20), 11767–11797. Re-
491 trieved from <https://acp.copernicus.org/articles/20/11767/2020/> doi:
492 10.5194/acp-20-11767-2020
- 493 Korolev, A., McFarquhar, G., Field, P. R., Franklin, C., Lawson, P., Wang, Z., ...
494 Wendisch, M. (2017). Mixed-phase clouds: Progress and challenges. *Me-*
495 *teorological Monographs*, 58, 5.1 - 5.50. Retrieved from [https://journals](https://journals.ametsoc.org/view/journals/amsm/58/1/amsmonographs-d-17-0001.1.xml)
496 [.ametsoc.org/view/journals/amsm/58/1/amsmonographs-d-17-0001.1.xml](https://journals.ametsoc.org/view/journals/amsm/58/1/amsmonographs-d-17-0001.1.xml)
497 doi: 10.1175/AMSMONOGRAPHS-D-17-0001.1
- 498 Lacher, L., DeMott, P. J., Levin, E. J. T., Suski, K. J., Boose, Y., Zipori, A., ...
499 Kanji, Z. A. (2018). Background free-tropospheric ice nucleating parti-
500 cle concentrations at mixed-phase cloud conditions. *Journal of Geophysical*
501 *Research: Atmospheres*, 123(18), 10,506-10,525. Retrieved from [https://](https://agupubs.onlinelibrary.wiley.com/doi/abs/10.1029/2018JD028338)
502 agupubs.onlinelibrary.wiley.com/doi/abs/10.1029/2018JD028338 doi:
503 <https://doi.org/10.1029/2018JD028338>
- 504 Lacher, L., Lohmann, U., Boose, Y., Zipori, A., Herrmann, E., Bukowiecki, N., ...
505 Kanji, Z. A. (2017). The horizontal ice nucleation chamber (hinc): Inp mea-
506 surements at conditions relevant for mixed-phase clouds at the high altitude
507 research station jungfrauoch. *Atmospheric Chemistry and Physics*, 17(24),
508 15199–15224. Retrieved from [https://acp.copernicus.org/articles/17/](https://acp.copernicus.org/articles/17/15199/2017/)
509 15199/2017/ doi: 10.5194/acp-17-15199-2017
- 510 Ladino, L. A., Korolev, A., Heckman, I., Wolde, M., Fridlind, A. M., & Ack-
511 erman, A. S. (2017). On the role of ice-nucleating aerosol in the for-
512 mation of ice particles in tropical mesoscale convective systems. *Geo-*
513 *physical Research Letters*, 44(3), 1574-1582. Retrieved from [https://](https://agupubs.onlinelibrary.wiley.com/doi/abs/10.1002/2016GL072455)
514 agupubs.onlinelibrary.wiley.com/doi/abs/10.1002/2016GL072455 doi:
515 <https://doi.org/10.1002/2016GL072455>
- 516 Lauber, A., Kiselev, A., Pander, T., Handmann, P., & Leisner, T. (2018). Sec-
517 ondary ice formation during freezing of levitated droplets. *Journal of*
518 *the Atmospheric Sciences*, 75(8), 2815 - 2826. Retrieved from [https://](https://journals.ametsoc.org/view/journals/atsc/75/8/jas-d-18-0052.1.xml)
519 journals.ametsoc.org/view/journals/atsc/75/8/jas-d-18-0052.1.xml
520 doi: 10.1175/JAS-D-18-0052.1

- 521 Mace, G. G., Benson, S., & Hu, Y. (2020). On the frequency of occurrence of the
522 ice phase in supercooled southern ocean low clouds derived from calipso and
523 cloudsat. *Geophysical Research Letters*, 47(14), e2020GL087554. Retrieved
524 from [https://agupubs.onlinelibrary.wiley.com/doi/abs/10.1029/](https://agupubs.onlinelibrary.wiley.com/doi/abs/10.1029/2020GL087554)
525 2020GL087554 (e2020GL087554 2020GL087554) doi: [https://doi.org/10.1029/](https://doi.org/10.1029/2020GL087554)
526 2020GL087554
- 527 Mace, G. G., Protat, A., & Benson, S. (2021). Mixed-phase clouds over the southern
528 ocean as observed from satellite and surface based lidar and radar. *Journal*
529 *of Geophysical Research: Atmospheres*, 126(16), e2021JD034569. Retrieved
530 from [https://agupubs.onlinelibrary.wiley.com/doi/abs/10.1029/](https://agupubs.onlinelibrary.wiley.com/doi/abs/10.1029/2021JD034569)
531 2021JD034569 (e2021JD034569 2021JD034569) doi: [https://doi.org/10.1029/](https://doi.org/10.1029/2021JD034569)
532 2021JD034569
- 533 McCluskey, C., Hill, T. C. J., Humphries, R. S., Rauker, A. M., Moreau, S., Strut-
534 ton, P. G., ... DeMott, P. J. (2018). Observations of ice nucleating particles
535 over southern ocean waters. *Geophysical Research Letters*, 45(21), 11,989-
536 11,997. Retrieved from [https://agupubs.onlinelibrary.wiley.com/doi/](https://agupubs.onlinelibrary.wiley.com/doi/abs/10.1029/2018GL079981)
537 abs/10.1029/2018GL079981 doi: <https://doi.org/10.1029/2018GL079981>
- 538 McCluskey, C. S., DeMott, P. J., Ma, P.-L., & Burrows, S. M. (2019). Nu-
539 merical representations of marine ice-nucleating particles in remote marine
540 environments evaluated against observations. *Geophysical Research Let-*
541 *ters*, 46(13), 7838-7847. Retrieved from [https://agupubs.onlinelibrary](https://agupubs.onlinelibrary.wiley.com/doi/abs/10.1029/2018GL081861)
542 [.wiley.com/doi/abs/10.1029/2018GL081861](https://agupubs.onlinelibrary.wiley.com/doi/abs/10.1029/2018GL081861) doi: [https://doi.org/10.1029/](https://doi.org/10.1029/2018GL081861)
543 2018GL081861
- 544 McCluskey, C. S., Ovadnevaite, J., Rinaldi, M., Atkinson, J., Belosi, F., Ceburnis,
545 D., ... DeMott, P. J. (2018). Marine and terrestrial organic ice-nucleating
546 particles in pristine marine to continentally influenced northeast atlantic air
547 masses. *Journal of Geophysical Research: Atmospheres*, 123(11), 6196-6212.
548 Retrieved from [https://agupubs.onlinelibrary.wiley.com/doi/abs/](https://agupubs.onlinelibrary.wiley.com/doi/abs/10.1029/2017JD028033)
549 10.1029/2017JD028033 doi: <https://doi.org/10.1029/2017JD028033>
- 550 Melsheimer, C., & Spreen, G. (2019a). *AMSR2 ASI sea ice concentration data,*
551 *Antarctic, version 5.4 (NetCDF) (July 2012 - December 2019)* [data set].
552 PANGAEA. Retrieved from <https://doi.org/10.1594/PANGAEA.898400>
553 doi: 10.1594/PANGAEA.898400
- 554 Melsheimer, C., & Spreen, G. (2019b). *AMSR2 ASI sea ice concentration data, Arc-*
555 *tic, version 5.4 (NetCDF) (July 2012 - December 2019)* [data set]. PANGAEA.
556 Retrieved from <https://doi.org/10.1594/PANGAEA.898399> doi: 10.1594/
557 PANGAEA.898399
- 558 Melsheimer, C., & Spreen, G. (2020a). *AMSR-E ASI sea ice concentration data,*
559 *Antarctic, version 5.4 (NetCDF) (June 2002 - September 2011)* [data set].
560 PANGAEA. Retrieved from <https://doi.org/10.1594/PANGAEA.919778>
561 doi: 10.1594/PANGAEA.919778
- 562 Melsheimer, C., & Spreen, G. (2020b). *AMSR-E ASI sea ice concentration data,*
563 *Arctic, version 5.4 (NetCDF) (June 2002 - September 2011)* [data set]. PAN-
564 GAEA. Retrieved from <https://doi.org/10.1594/PANGAEA.919777> doi: 10
565 .1594/PANGAEA.919777
- 566 Meyers, M. P., DeMott, P. J., & Cotton, W. R. (1992). New primary ice-
567 nucleation parameterizations in an explicit cloud model. *Journal of Ap-*
568 *plied Meteorology and Climatology*, 31(7), 708 - 721. Retrieved from
569 [https://journals.ametsoc.org/view/journals/apme/31/7/1520-0450](https://journals.ametsoc.org/view/journals/apme/31/7/1520-0450_1992_031_0708_npipni_2_0_co_2.xml)
570 [_1992_031_0708_npipni_2_0_co_2.xml](https://journals.ametsoc.org/view/journals/apme/31/7/1520-0450_1992_031_0708_npipni_2_0_co_2.xml) doi: 10.1175/1520-0450(1992)031<0708:
571 NPINPI>2.0.CO;2
- 572 Mignani, C., Creamean, J. M., Zimmermann, L., Alewell, C., & Conen, F. (2019).
573 New type of evidence for secondary ice formation at around -15c in mixed-
574 phase clouds. *Atmospheric Chemistry and Physics*, 19(2), 877-886. Re-
575 trieved from <https://acp.copernicus.org/articles/19/877/2019/> doi:

- 10.5194/acp-19-877-2019
- Murray, B. J., Carslaw, K. S., & Field, P. R. (2021). Opinion: Cloud-phase climate feedback and the importance of ice-nucleating particles. *Atmospheric Chemistry and Physics*, 21(2), 665–679. Retrieved from <https://acp.copernicus.org/articles/21/665/2021/> doi: 10.5194/acp-21-665-2021
- Murray, B. J., O’Sullivan, D., Atkinson, J. D., & Webb, M. E. (2012). Ice nucleation by particles immersed in supercooled cloud droplets. *Chem. Soc. Rev.*, 41, 6519–6554. Retrieved from <http://dx.doi.org/10.1039/C2CS35200A> doi: 10.1039/C2CS35200A
- Palm, S. P., Strey, S. T., Spinhirne, J., & Markus, T. (2010). Influence of arctic sea ice extent on polar cloud fraction and vertical structure and implications for regional climate. *Journal of Geophysical Research: Atmospheres*, 115(D21). Retrieved from <https://agupubs.onlinelibrary.wiley.com/doi/abs/10.1029/2010JD013900> doi: <https://doi.org/10.1029/2010JD013900>
- Petters, M. D., & Wright, T. P. (2015). Revisiting ice nucleation from precipitation samples. *Geophysical Research Letters*, 42(20), 8758–8766. Retrieved from <https://agupubs.onlinelibrary.wiley.com/doi/abs/10.1002/2015GL065733> doi: <https://doi.org/10.1002/2015GL065733>
- Pratt, K., DeMott, P., French, J., Wang, Z., Westphal, D., Heymsfield, A., ... Prather, K. (2009, 05). In situ detection of biological particles in cloud ice-crystals. *Nature Geoscience*, 2, 398–401. doi: 10.1038/NGEO521
- Prenni, A. J., Harrington, J. Y., Tjernström, M., DeMott, P. J., Avramov, A., Long, C. N., ... Verlinde, J. (2007). Can ice-nucleating aerosols affect arctic seasonal climate? *Bulletin of the American Meteorological Society*, 88(4), 541 – 550. Retrieved from <https://journals.ametsoc.org/view/journals/bams/88/4/bams-88-4-541.xml> doi: 10.1175/BAMS-88-4-541
- Ramelli, F., Henneberger, J., David, R. O., Bühl, J., Radenz, M., Seifert, P., ... Lohmann, U. (2021). Microphysical investigation of the seeder and feeder region of an alpine mixed-phase cloud. *Atmospheric Chemistry and Physics*, 21(9), 6681–6706. Retrieved from <https://acp.copernicus.org/articles/21/6681/2021/> doi: 10.5194/acp-21-6681-2021
- Rangno, A. L., & Hobbs, P. V. (2001). Ice particles in stratiform clouds in the arctic and possible mechanisms for the production of high ice concentrations. *Journal of Geophysical Research: Atmospheres*, 106(D14), 15065–15075. Retrieved from <https://agupubs.onlinelibrary.wiley.com/doi/abs/10.1029/2000JD900286> doi: <https://doi.org/10.1029/2000JD900286>
- Rinaldi, M., Hiranuma, N., Santachiara, G., Mazzola, M., Mansour, K., Paglione, M., ... Belosi, F. (2021). Ice-nucleating particle concentration measurements from ny-ålesund during the arctic spring–summer in 2018. *Atmospheric Chemistry and Physics*, 21(19), 14725–14748. Retrieved from <https://acp.copernicus.org/articles/21/14725/2021/> doi: 10.5194/acp-21-14725-2021
- Rogers, D. C., DeMott, P. J., & Kreidenweis, S. M. (2001). Airborne measurements of tropospheric ice-nucleating aerosol particles in the arctic spring. *Journal of Geophysical Research: Atmospheres*, 106(D14), 15053–15063. Retrieved from <https://agupubs.onlinelibrary.wiley.com/doi/abs/10.1029/2000JD900790> doi: <https://doi.org/10.1029/2000JD900790>
- Sanchez-Marroquin, A., Arnalds, O., Baustian-Dorsi, K. J., Browse, J., Dagsson-Waldhauserova, P., Harrison, A. D., ... Murray, B. J. (2020). Iceland is an episodic source of atmospheric ice-nucleating particles relevant for mixed-phase clouds. *Science Advances*, 6(26), eaba8137. Retrieved from <https://www.science.org/doi/abs/10.1126/sciadv.aba8137> doi: 10.1126/sciadv.aba8137
- Sassen, K., Wang, Z., & Liu, D. (2008). Global distribution of cirrus clouds from cloudsat/cloud-aerosol lidar and infrared pathfinder satellite observations

- (calipso) measurements. *Journal of Geophysical Research: Atmospheres*, 113(D8). Retrieved from <https://agupubs.onlinelibrary.wiley.com/doi/abs/10.1029/2008JD009972> doi: <https://doi.org/10.1029/2008JD009972>
- Schneider, J., Höhler, K., Heikkilä, P., Keskinen, J., Bertozzi, B., Bogert, P., ... Möhler, O. (2021). The seasonal cycle of ice-nucleating particles linked to the abundance of biogenic aerosol in boreal forests. *Atmospheric Chemistry and Physics*, 21(5), 3899–3918. Retrieved from <https://acp.copernicus.org/articles/21/3899/2021/> doi: 10.5194/acp-21-3899-2021
- Schnell, R. C. (1977). Ice nuclei in seawater, fog water and marine air off the coast of nova scotia: Summer 1975. *Journal of Atmospheric Sciences*, 34(8), 1299 - 1305. Retrieved from https://journals.ametsoc.org/view/journals/atsc/34/8/1520-0469_1977_034_1299_inisfw_2_0_co_2.xml doi: 10.1175/1520-0469(1977)034<1299:INISFW>2.0.CO;2
- Schnell, R. C., & Vali, G. (1975). Freezing nuclei in marine waters. *Tellus*, 27(3), 321–323. Retrieved from <https://doi.org/10.3402/tellusa.v27i3.9911> doi: 10.3402/tellusa.v27i3.9911
- Sotiropoulou, G., Tjernström, M., Sedlar, J., Achtert, P., Brooks, B. J., Brooks, I. M., ... Wolfe, D. (2016). Atmospheric conditions during the arctic clouds in summer experiment (acse): Contrasting open water and sea ice surfaces during melt and freeze-up seasons. *Journal of Climate*, 29(24), 8721 - 8744. Retrieved from <https://journals.ametsoc.org/view/journals/clim/29/24/jcli-d-16-0211.1.xml> doi: 10.1175/JCLI-D-16-0211.1
- Spren, G., Kaleschke, L., & Heygster, G. (2008). Sea ice remote sensing using amsr-e 89-ghz channels. *Journal of Geophysical Research: Oceans*, 113(C2). Retrieved from <https://agupubs.onlinelibrary.wiley.com/doi/abs/10.1029/2005JC003384> doi: <https://doi.org/10.1029/2005JC003384>
- Stephens, G. L., Vane, D. G., Boain, R. J., Mace, G. G., Sassen, K., Wang, Z., ... the CloudSat Science Team (2002). The cloudsat mission and the a-train: A new dimension of space-based observations of clouds and precipitation. *Bulletin of the American Meteorological Society*, 83(12), 1771 - 1790. Retrieved from <https://journals.ametsoc.org/view/journals/bams/83/12/bams-83-12-1771.xml> doi: 10.1175/BAMS-83-12-1771
- Stopelli, E., Conen, F., Morris, C., Herrmann, E., Bukowiecki, N., & Alewell, C. (2015, 11). Ice nucleation active particles are efficiently removed by precipitating clouds. *Scientific Reports*, 5, 16433. doi: 10.1038/srep16433
- Tan, I., Storelvmo, T., & Choi, Y.-S. (2014). Spaceborne lidar observations of the ice-nucleating potential of dust, polluted dust, and smoke aerosols in mixed-phase clouds. *Journal of Geophysical Research: Atmospheres*, 119(11), 6653–6665. Retrieved from <https://agupubs.onlinelibrary.wiley.com/doi/abs/10.1002/2013JD021333> doi: <https://doi.org/10.1002/2013JD021333>
- Tan, I., Storelvmo, T., & Zelinka, M. D. (2016). Observational constraints on mixed-phase clouds imply higher climate sensitivity. *Science*, 352(6282), 224–227. Retrieved from <https://www.science.org/doi/abs/10.1126/science.aad5300> doi: 10.1126/science.aad5300
- Tobo, Y., Adachi, K., DeMott, P., Hill, T., Hamilton, D., Mahowald, N., ... Koike, M. (2019, 04). Glacially sourced dust as a potentially significant source of ice nucleating particles. *Nature Geoscience*, 12, 1–6. doi: 10.1038/s41561-019-0314-x
- Vali, G. (1971). Supercooling of water and nucleation of ice (drop freezer). *American Journal of Physics*, 39, 1125–1128.
- Vergara-Temprado, J., Miltenberger, A. K., Furtado, K., Grosvenor, D. P., Shipway, B. J., Hill, A. A., ... Carslaw, K. S. (2018). Strong control of southern ocean cloud reflectivity by ice-nucleating particles. *Proceedings of the National Academy of Sciences*, 115(11), 2687–2692. Retrieved from <https://www.pnas.org/content/115/11/2687> doi: 10.1073/pnas.1721627115

- 686 Vonnegut, B. (1947). The nucleation of ice formation by silver iodide. *Journal of*
687 *Applied Physics*, 18(7), 593-595. Retrieved from [https://doi.org/10.1063/1](https://doi.org/10.1063/1.1697813)
688 .1697813 doi: 10.1063/1.1697813
- 689 Wang, Z. (2019). Cloudsat 2b-cldclass-lidar product process description and inter-
690 face control document [Computer software manual].
- 691 Welti, A., Bigg, E. K., DeMott, P. J., Gong, X., Hartmann, M., Harvey, M.,
692 ... Stratmann, F. (2020). Ship-based measurements of ice nuclei con-
693 centrations over the arctic, atlantic, pacific and southern oceans. *At-*
694 *mospheric Chemistry and Physics*, 20(23), 15191–15206. Retrieved
695 from <https://acp.copernicus.org/articles/20/15191/2020/> doi:
696 10.5194/acp-20-15191-2020
- 697 Wex, H., Huang, L., Zhang, W., Hung, H., Traversi, R., Becagli, S., ... Stratmann,
698 F. (2019). Annual variability of ice-nucleating particle concentrations at dif-
699 ferent arctic locations. *Atmospheric Chemistry and Physics*, 19(7), 5293–5311.
700 Retrieved from <https://acp.copernicus.org/articles/19/5293/2019/>
701 doi: 10.5194/acp-19-5293-2019
- 702 Wilson, T., Ladino, L., Alpert, P., Breckels, M., Brooks, I., Browse, J., ... Murray,
703 B. (2015, 09). A marine biogenic source of atmospheric ice-nucleating particles.
704 *Nature*, 525, 234. doi: 10.1038/nature14986
- 705 Winker, D. M., Hunt, W. H., & McGill, M. J. (2007). Initial performance assess-
706 ment of calip. *Geophysical Research Letters*, 34(19). Retrieved from [https://](https://agupubs.onlinelibrary.wiley.com/doi/abs/10.1029/2007GL030135)
707 agupubs.onlinelibrary.wiley.com/doi/abs/10.1029/2007GL030135 doi:
708 <https://doi.org/10.1029/2007GL030135>
- 709 Winker, D. M., Pelon, J., Coakley, J. A., Ackerman, S. A., Charlson, R. J., Co-
710 larco, P. R., ... Wielicki, B. A. (2010). The calipso mission: A global 3d
711 view of aerosols and clouds. *Bulletin of the American Meteorological Society*,
712 91(9), 1211 - 1230. Retrieved from [https://journals.ametsoc.org/view/](https://journals.ametsoc.org/view/journals/bams/91/9/2010bams3009.1.xml)
713 journals/bams/91/9/2010bams3009.1.xml doi: 10.1175/2010BAMS3009.1
- 714 Young, G., Connolly, P. J., Jones, H. M., & Choulaton, T. W. (2017). Microphysi-
715 cal sensitivity of coupled springtime arctic stratocumulus to modelled primary
716 ice over the ice pack, marginal ice, and ocean. *Atmospheric Chemistry and*
717 *Physics*, 17(6), 4209–4227. Retrieved from [https://acp.copernicus.org/](https://acp.copernicus.org/articles/17/4209/2017/)
718 [articles/17/4209/2017/](https://acp.copernicus.org/articles/17/4209/2017/) doi: 10.5194/acp-17-4209-2017
- 719 Zelinka, M. D., Myers, T. A., McCoy, D. T., Po-Chedley, S., Caldwell, P. M.,
720 Ceppi, P., ... Taylor, K. E. (2020). Causes of higher climate sensitivity
721 in cmip6 models. *Geophysical Research Letters*, 47(1), e2019GL085782.
722 Retrieved from [https://agupubs.onlinelibrary.wiley.com/doi/abs/](https://agupubs.onlinelibrary.wiley.com/doi/abs/10.1029/2019GL085782)
723 [10.1029/2019GL085782](https://agupubs.onlinelibrary.wiley.com/doi/abs/10.1029/2019GL085782) (e2019GL085782 10.1029/2019GL085782) doi:
724 <https://doi.org/10.1029/2019GL085782>
- 725 Zhang, D., Wang, Z., & Liu, D. (2010). A global view of midlevel liquid-layer
726 topped stratiform cloud distribution and phase partition from calipso and
727 cloudsat measurements. *Journal of Geophysical Research: Atmospheres*,
728 115(D4). Retrieved from [https://agupubs.onlinelibrary.wiley.com/doi/](https://agupubs.onlinelibrary.wiley.com/doi/abs/10.1029/2009JD012143)
729 [abs/10.1029/2009JD012143](https://agupubs.onlinelibrary.wiley.com/doi/abs/10.1029/2009JD012143) doi: <https://doi.org/10.1029/2009JD012143>